Applied Catalysis B: Environmental 98 (2010) 180–185

Contents lists available at ScienceDirect

Applied Catalysis B: Environmental

journal homepage: www.elsevier.com/locate/apcatb

Catalytic combustion of VOCs over a series of manganese oxide catalysts

Sang Chai Kim [a,*], Wang Geun Shim [b]

[a] Department of Environmental Education, Mokpo National University, 61, Dorim Ri, Cheonggye Myeon, Muan 534-729, Republic of Korea
[b] School of Applied Chemical Engineering, Chonnam National University, 300, Yongbong Dong, Buk-Ku, Gwangju 500-757, Republic of Korea

ARTICLE INFO

Article history:
Received 24 February 2010
Received in revised form 25 May 2010
Accepted 25 May 2010
Available online 1 June 2010

Keywords:
Catalytic combustion
Manganese oxide
Alkaline metal
Alkaline earth metal
Promoter

ABSTRACT

Catalytic combustion of volatile organic compounds (VOCs: benzene and toluene) was studied over manganese oxide catalysts (Mn_3O_4, Mn_2O_3 and MnO_2) and over the promoted manganese oxide catalysts with alkaline metal and alkaline earth metal. Their properties and performance were characterized by using the Brunauer Emmett Teller (BET), temperature programmed reduction (TPR), X-ray diffraction (XRD) and X-ray photoelectron spectroscopy (XPS). The sequence of catalytic activity was as follows: $Mn_3O_4 > Mn_2O_3 > MnO_2$, which was correlated with the oxygen mobility on the catalyst. Each addition of potassium (K), calcium (Ca) and magnesium (Mg) to Mn_3O_4 catalyst enhanced the catalytic activity of Mn_3O_4 catalyst. Accordingly, K, Ca and Mg seemed to act as promoters, and the promoting effect might be ascribed to the defect-oxide or a hydroxyl-like group. A mutual inhibitory effect was observed between benzene and toluene in the binary mixture. In addition, the order of catalytic activity with respect to VOC molecules for single compound is benzene > toluene, and the binary mixture showed the opposite order of toluene > benzene.

1. Introduction

Volatile organic compounds (VOCs) are not only hazardous air pollutants because of their toxic, malodorous, mutagenic and carcinogenic nature, but they are also ozone and smog precursors [1–3]. Catalytic oxidation is recognized as a potent method of controlling emissions of VOCs owing to its low thermal NO_x emissions, low operating cost, and high destructive efficiency [4,5]. At present, supported noble metals (Pt and Pd) [6–10] and metal oxides catalysts [11–13] are used for reduction of VOCs emissions. Especially, transition metal oxides have shown a very good catalytic performance in oxidation reactions. Moreover, they have lower costs and higher resistance to poisons [13,14].

Manganese oxides such as Mn_3O_4 [15], Mn_2O_3 [16] and MnO_2 [17] are known for exhibiting high activity in the oxidation of hydrocarbons. Recently, Ramesh et al. [18] have reported that the reactivity shows an order of $MnO \leq MnO_2 < Mn_2O_3$ in the CO oxidation. Santos et al. [19] have reported that manganese oxides are actively involved in complete oxidation of ethyl acetate, which is oxidized into CO_2 at temperatures below 250 °C. Their catalytic application is due to their high efficiency in the reaction/oxidation cycles. Redox capabilities are strongly enhanced when combined with other elements [20]. Also, manganese oxides are considered as environmentally friendly materials [21]. Tseng and Chu [22] have reported MnO/Fe_2O_3 was excellent metal oxide catalyst in the catalytic oxidation of styrene. Bastos et al. [23] have found a strong correlation between the catalytic activity and the lattice oxygen donating ability over manganese oxides which were synthesized by exotemplating using an activated carbon and a carbon xerogel as templates for the total oxidation of ethanol. Gandhe et al. [5] have showed that presence of Mn^{4+}/Mn^{3+} type redox couples and facile lattice oxygen on manganese oxide OMS-2 catalyst had an important role in total oxidation of ethyl acetate. It has been reported that the presence of alkali and alkaline earth metal oxides in marine manganese nodules may act as promoter in some base-catalyzed reactions [24].

The aim of this work are to systematically analyze the catalytic properties and performance of manganese oxides in oxidizing VOCs, and examine the effect of adding alkali (K) and alkaline earth metal (Ca, Mg) to manganese oxide catalyst on the catalytic activity. The changes in the physicochemical states of the catalysts were also examined by using the BET, XRD, TPR and XPS.

2. Experimental

2.1. Catalysts

Manganese oxides and precursors of promoters were purchased from Aldrich chemical company. Mn_3O_4, Mn_2O_3 and MnO_2 (0.12–0.16 mm) were used after treating with calcinations at 400 °C for 6 h. In addition the promoted Mn_3O_4 catalysts were prepared with potassium nitrate, calcium carbonate and magnesium nitrate

* Corresponding author. Tel.: +82 61 450 2781; fax: +82 61 450 2780.
E-mail address: gikim@mokpo.ac.kr (S.C. Kim).

0926-3373/$ – see front matter © 2010 Published by Elsevier B.V.
doi:10.1016/j.apcatb.2010.05.027

mixed deionized water taken in appropriate ratio. Resulting materials were vaporized with stirring at 90 °C and then dried at 120 °C overnight, followed by calcinations at 400 °C for 6 h.

2.2. Characterization of catalysts

The Brunauer Emmett Teller (BET) surface areas of the catalysts were determined by nitrogen adsorption at 77 K using a Micromeritics ASAP 2020 analyzer. The crystal structures of samples used in this work were examined by X-ray diffraction (XRD) data using a Phillips PW3123 diffractometer equipped with a graphite monochrometer and Cu Kα radiation of wavelength 0.154 nm. The samples used were investigated in the 2 range of 20–90° at a scanning speed of 70° h^{-1}. The measured XRD patterns were compared with the ICDD file. X-ray photoelectron spectrometer (XPS) analysis was conducted using a photoelectron spectrometer VG Scientific MultiLab 2000 system equipped with a non-monochromatic Mg Kα radiation of 1253.6 eV. The C 1s peak (285 eV) was used for the calibration of binding energy values. The pressure in the analytical chamber was about 10^{-9} Pa. Temperature programmed reduction (TPR) was performed using ChemBET 3000 (Quantrachrome) setup. The gas mixture (10% H_2 and 90% N_2) was passed through the catalyst sample (0.2 g) at a rate of 60 ml/min, while the temperature was increased up to 600 °C at a rate of 10 °C/min.

2.3. Catalytic oxidation

The catalytic oxidations were carried out using a conventional fixed bed flow reactor. The reactor has three major sections: (1) apparatus for preparation of vapors, (2) fixed bed flow reactor in a heating system, and (3) apparatus for the analysis of reactants and products.

The catalytic reactor (quartz tube with the shape of a I) was consisted of a vertical tubular with 1.0 cm diameter and 35 cm length in an electrical heating system controlled by a proportional integral derivative (PID) controller. In order to get an accurate measurement of the catalyst temperature, K type thermocouple was positioned in the catalyst bed. A catalyst sample of 0.4 g was loaded in the middle of the reactor supported by quartz wool. Benzene and toluene were purchased from Fisher and used without further treatment. An air stream bubbling through a saturator filled with liquid hydrocarbon carried an individual vapor. For accurate and stable controlling the gas flow rates, mass flow controllers (UNIT Instrument, UFC-8100) were employed. The concentration of benzene and toluene were 1000 ppm (2000 ppm), respectively, controlled by the temperature of the saturator and mixed with another air stream. The flow rate of gas mixture through the reactor was 100 STP cm^3/min. All lines were heated sufficiently at 120 °C to prevent the adsorption and condensation of reactant and product in the tubes. Experimental data were collected after ensuring the steady state condition in each step.

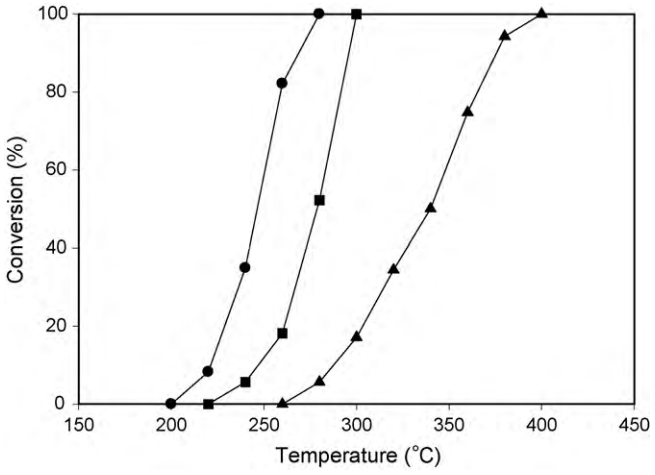

Fig. 1. Toluene conversion over manganese oxide catalysts. *Reaction condition*: catalyst weight = 0.4 g; toluene concentration = 1000 ppm; total flow rate = 100 cm^3/min. (●) Mn_3O_4; (■) Mn_2O_3; (▲) MnO_2.

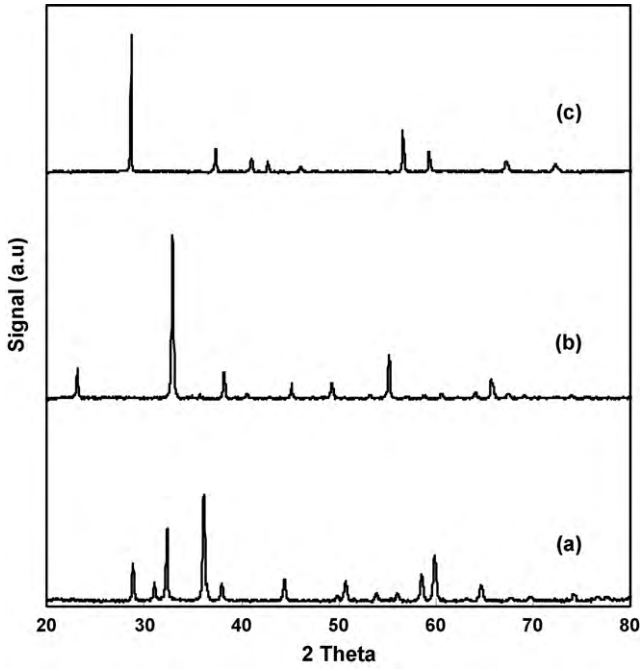

Fig. 2. XRD patterns of manganese oxide catalysts. (a) Mn_3O_4, (b) Mn_2O_3, and (c) MnO_2.

The concentration of inlet and exit gas stream was determined using a gas chromatograph, GC-14A model (Shimadzu) equipped with thermal conductivity. The chromatographic column used was composed of a 5% bentone-34 and 5%DNP/simalite (60–80 mesh, 3 mm Ø × 3 m) for toluene analysis, and a porapak Q (50–80 mesh, 3 mm Ø × 3 m) was used for CO_2 separation. The GC/MS (Shimadzu, QP5050) was also employed for the quantitative and qualitative analysis of the products and by-products. In the present work, the only products were CO_2 and H_2O and other by-products were not found under most experimental conditions. Thus, the conversion was calculated based on hydrocarbon consumption.

3. Results and discussion

3.1. Manganese oxides

Toluene conversion was measured as a function of reaction temperature over Mn_3O_4, Mn_2O_3 and MnO_2 catalysts as shown in Fig. 1. The catalytic activities of these catalysts are in the order $Mn_3O_4 > Mn_2O_3 > MnO_2$ according to the conversion profiles. For example, reaction temperatures for T_{50} conversion (the value of the temperature at conversion approaches 50%) and T_{90} conversion (the value of the temperature at conversion approaches 90%) of toluene over the three manganese oxide catalysts are 245 and 270 °C for Mn_3O_4, 280 and 295 °C for Mn_2O_3, and 340 and 375 °C for MnO_2. This experimental result reveals that the catalytic activity is apparently dependent on the oxidation state of manganese.

The XRD and the BET surface area measurements were carried out to examine the properties of the manganese oxide catalysts. Fig. 2 presents the XRD patterns of these catalysts. The XRD pro-

Table 1
BET surface area, TPR data and T_{90} of manganese oxide catalysts.

Name	Mn_3O_4	Mn_2O_3	MnO_2
BET surface area (m^2/g)	18	7	3
Starting reduction temperature (°C)	170	305	311
Temperature of TPR peak (°C)	293[a], 460[b]	403[a], 515[b]	391[a], 625[b]
End of reduction temperature (°C)	545	610	–
T_{90} (°C)	270	295	375

[a] 1st peak.
[b] 2nd peak.

files of manganese oxide catalysts revealed the diffraction peak of Mn_3O_4 crystalline phase (hausmanite) which reflected only the Mn_3O_4 catalyst, the peak of Mn_2O_3 crystalline phase (alpha) which reflected only the Mn_2O_3 catalyst, and the peak of MnO_2 crystalline phase (beta) which reflected only the MnO_2 catalyst. Accordingly, each manganese oxide catalyst is in full accord with each manganese oxide crystalline phase. We compared the BET surface areas of manganese oxide catalysts, and the result is listed in Table 1. The BET surface areas of Mn_3O_4, Mn_2O_3 and MnO_2 are 18, 7 and 3 m^2/g, respectively. This result indicates that the order of catalytic activities of the three manganese oxide catalysts is highly correlated with that of the BET surface areas. In other words, the higher the BET surface areas, the higher the catalytic activity.

Fig. 3 shows the TPR profiles of three manganese oxide catalysts with different oxidation states, and the temperatures of TPR peak (TTP) for them are summarized in Table 1. As can be seen in Fig. 3, the TPR patterns strongly depend on the oxidation state of the catalyst. Mn_3O_4 catalyst shows two main reduction peaks of which first reduction peak (TTP: 293 °C) is greater than the second reduction peak (TTP: 460 °C). This result is in good accordance with Yongnian et al.'s one [25]. They have reported that Mn_3O_4 has a normal spinel structure with Mn^{2+} ions in tetrahedral sites and Mn^{3+} ions in tetragonally distorted octahedral sites [26], and a nonstoichiometric Mn_3O_4 has a nonstoichiometric oxygen which should be bound to the tetrahedral Mn, thus consists of three kinds of Mn^{3+}–O bonds which are the octahedral long and short Mn^{3+}–O and the tetrahedral Mn^{3+}–O bonds, available in a nonstoichiometric Mn_3O_4. Furthermore, they deduced that the increasing degrees of difficulty in the reduction of different Mn^{3+}–O to MnO may be as follows: tetrahedral Mn^{3+} < octahedral long Mn^{3+} ∼ octahedral short

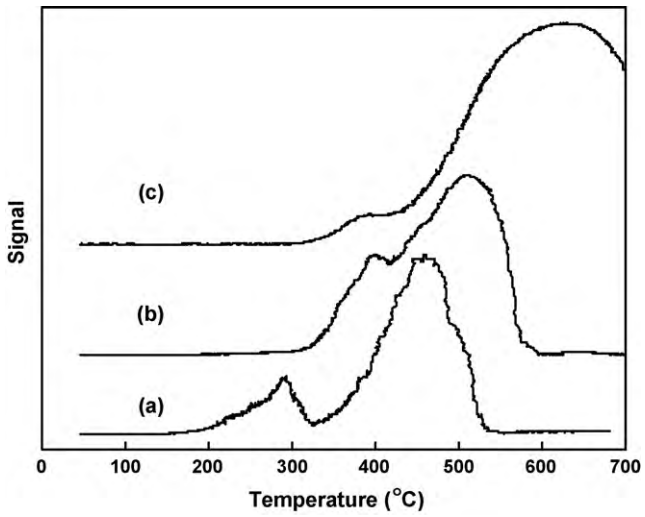

Fig. 3. TPR profiles of manganese oxide catalysts. (a) Mn_3O_4, (b) Mn_2O_3, and (c) MnO_2.

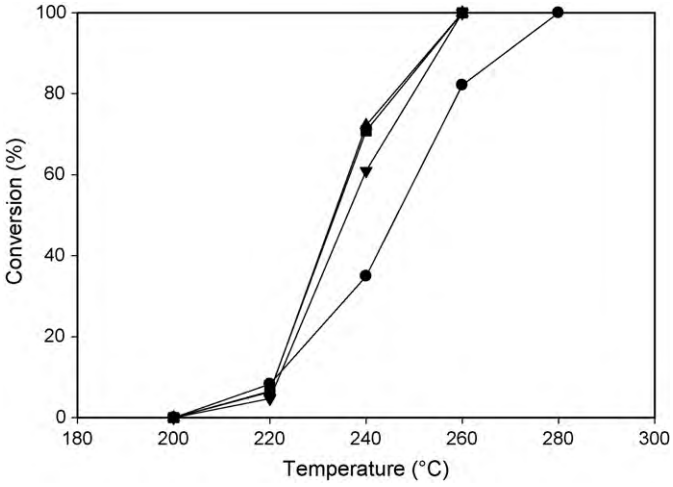

Fig. 4. Toluene conversion over the promoted Mn_3O_4 catalysts with K, Ca and Mg. *Reaction condition*: catalyst weight = 0.4 g; toluene concentration = 1000 ppm; total flow rate = 100 cm^3/min. (●) Mn_3O_4; (■) 0.5 wt% K/Mn_3O_4; (▲) 0.5 wt% Ca/Mn_3O_4; (▼) 0.5 wt% Mg/Mn_3O_4.

Mn^{3+} or octahedral long Mn^{3+} < tetrahedral Mn^{3+} ∼ octahederal short Mn^{3+}. Accordingly, it was concluded that the first reduction peak is due to the tetrahedral Mn^{3+} or octahedral long Mn^{3+} and the second one can be assigned to the co-reduction of octahedral short Mn^{3+} with octahedral long Mn^{3+} or tetrahedral Mn^{3+}. The TPR profile of Mn_2O_3 catalyst shows one main peak at 515 °C ($Mn_3O_4 \rightarrow MnO$) with a shoulder at 403 °C ($Mn_2O_3 \rightarrow Mn_3O_4$). The profile of MnO_2 catalyst too exhibits two reduction peak of which the second reduction peak (625 °C) is much greater than the first one (391 °C). Christel et al. [27] have reported that MnO_2 is successively reduced as follows: $MnO_2 \rightarrow Mn_2O_3 \rightarrow Mn_3O_4 \rightarrow MnO$, thus has three reduction peaks. Accordingly, as shown in Fig. 3(c), the first reduction peak is due to MnO_2 and the second reduction peak seems to be attributed to the simultaneous reductions of Mn_2O_3 and Mn_3O_4. The TPR results indicate that MnO_2 exhibits the highest TTP, followed in order by Mn_2O_3 and Mn_3O_4. The reduction temperature shifting to higher temperature means the decrease in the lattice oxygen mobility on the catalyst. Therefore, the catalytic activity of toluene oxidation appears to be correlated with the oxygen mobility [28,29]. In other words, the higher the oxygen mobility, the higher the catalytic activity.

3.2. Effect of promoter (K, Ca and Mg)

The conversion profiles were measured with toluene conversion as a function of reaction temperature over 0.5 wt% K/Mn_3O_4, 0.5 wt% Ca/Mn_3O_4 and 0.5 wt% Mg/Mn_3O_4 catalysts as shown in Fig. 4. The conversion profiles for these samples shift to lower temperatures compared to that for Mn_3O_4 catalyst. For example, the reaction temperatures for T_{50} (T_{90}) conversion of toluene over 0.5 wt% K/Mn_3O_4, 0.5 wt% Ca/Mn_3O_4 and 0.5 wt% Mg/Mn_3O_4 catalysts, are 230 (250), 230 (250) and 232 (255) °C, respectively. This result indicates that that the additions of K, Ca and Mg to Mn_3O_4 catalyst lead to enhance the catalytic activity, and subsequently, K, Ca and Mg act as promoters.

The XRD and the BET surface area measurements were carried out to examine the properties of the promoted Mn_3O_4 catalysts. The XRD patterns of these catalysts are presented in Fig. 5. The XRD profiles of the promoted Mn_3O_4 catalysts reveal only the diffraction peaks of Mn_3O_4 crystalline phases. The BET surface areas of the promoted Mn_3O_4 catalysts are summarized in Table 2. The BET surface areas for the parent and the promoted Mn_3O_4 catalysts are similar in the range of 16–17 $m^2\ g^{-1}$, within the experimental error.

Table 2
BET surface area, TPR data and T_{90} of Mn_3O_4 catalyst promoted with K, Ca and Mg.

Name	0.5 wt% K/Mn_3O_4	0.5 wt% Ca/Mn_3O_4	0.5 wt% Mg/Mn_3O_4
BET surface area (m^2/g)	16	16	17
Temperature of TPR peak (°C)	246[a], 296[b], 448[c]	234[a], 296[b], 489[c]	227[a], 296[b], 464[c]
T_{90} (°C)	250	250	255

[a] Shoulder peak.
[b] 1st peak.
[c] 2nd peak.

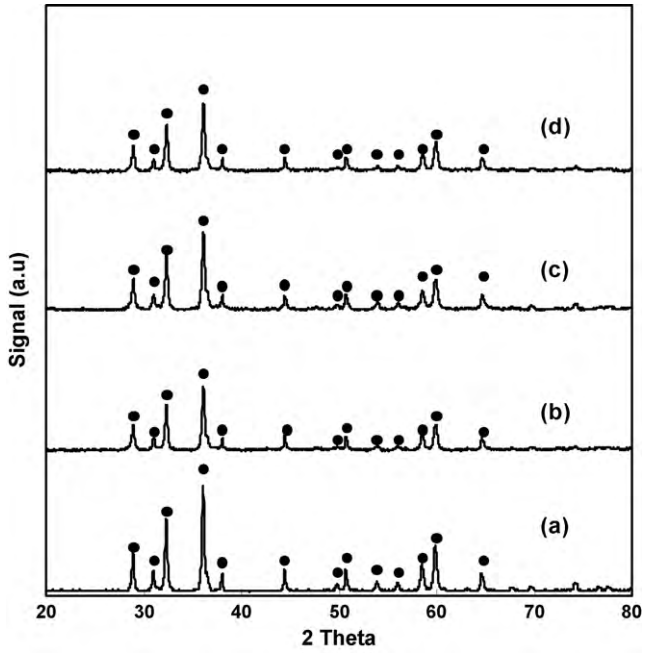

Fig. 5. XRD patterns of the promoted Mn_3O_4 catalysts with K, Ca and Mg. (a) Mn_3O_4, (b) 0.5 wt% K/Mn_3O_4, (c) 0.5 wt% Ca/Mn_3O_4, and (d) 0.5 wt% Mg/Mn_3O_4. (●) Mn_3O_4.

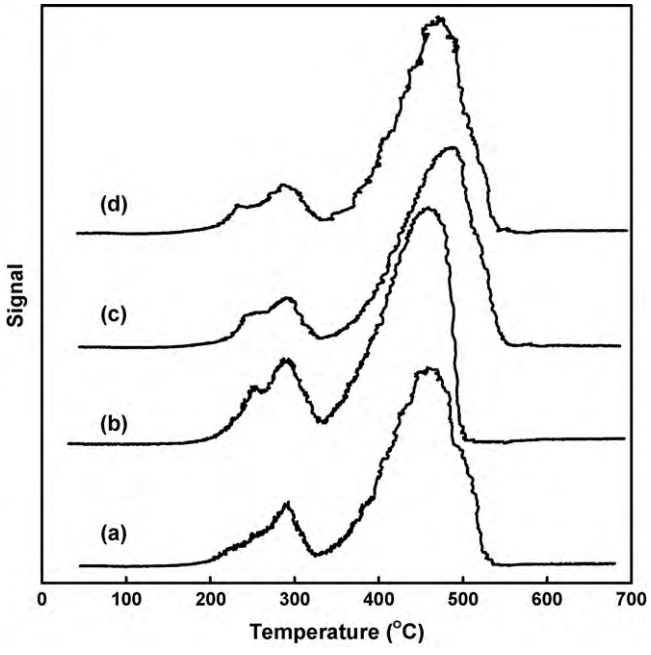

Fig. 6. TPR profiles of the promoted Mn_3O_4 catalysts with K, Ca and Mg. (a) Mn_3O_4, (b) 0.5 wt% K/Mn_3O_4, (c) 0.5 wt% Ca/Mn_3O_4, and (d) 0.5 wt% Mg/Mn_3O_4.

Table 3
Binding energies (BEs) of the Mn 2p for MnO_2, Mn_2O_3 and M_3O_4 catalysts.

Name	Mn_3O_4	Mn_2O_3	MnO_2
Mn $2p_3$ (eV)	641.01	642.19	642.61
Mn $2p_1$ (eV)	653.61	654.22	654.42

Fig. 6 shows the TPR profiles of the promoted Mn_3O_4 catalysts, and their TTPs are summarized in Table 2. The TPR profiles of 0.5 wt% K/Mn_3O_4, 0.5 wt% Ca/Mn_3O_4 and 0.5 wt% Mg/Mn_3O_4 catalysts show two main reduction peaks, which are similar to that of the parent catalyst. However, it was observed that new shoulder peaks appear at the reduction temperature ranging from 227 to 234 °C in the promoted Mn_3O_4 catalysts. Accordingly, the increase in catalytic activity of the promoted Mn_3O_4 catalyst seems to be related to this shoulder peak.

3.3. XPS analysis

The oxidation states of surface species on MnO_2, Mn_2O_3, Mn_3O_4 and the promoted Mn_3O_4 catalysts were characterized by an XPS analysis. The binding energies (BEs) of Mn 2p for manganese oxide catalysts are summarized in Table 3. The BEs of Mn $2p_3$ (Mn $2P_1$) of MnO_2, Mn_2O_3 and Mn_3O_4 are 642.61 (653.16), 642.19 (654.22) and 641.01 (654.42) eV, respectively.

Figs. 7 and 8 represent the evolution of XPS spectra of Mn 2p and O 1s core levels for Mn_3O_4 and the promoted Mn_3O_4, respectively. In addition, the binding energies (BEs) of Mn 2p and O 1s are summarized in Table 4. As shown in Table 4, the additions of K, Ca

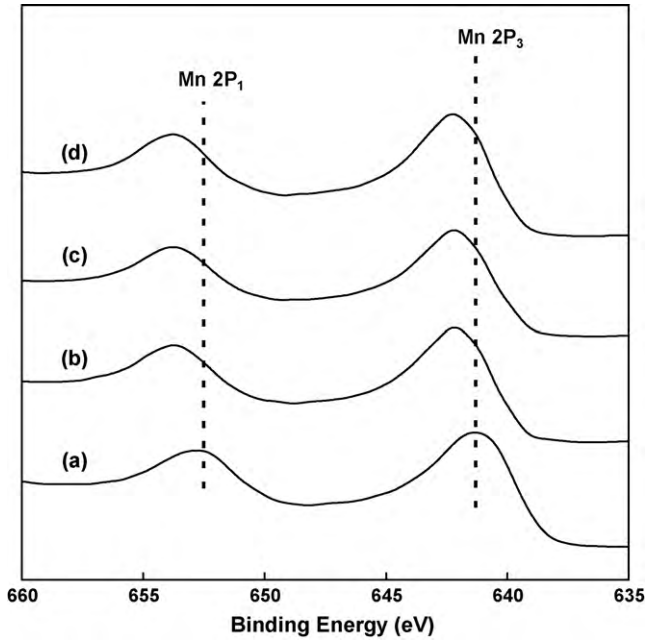

Fig. 7. XPS spectra of the Mn 2p region of samples. (a) Mn_3O_4, (b) 0.5 wt% K/Mn_3O_4, (c) 0.5 wt% Ca/Mn_3O_4, and (d) 0.5 wt% Mg/Mn_3O_4.

Table 4
Binding energies (BEs) of the Mn $2p_3$, the O 1s A and O 1s B, and the area ratios of O 1s B/O 1s A for the catalysts.

Name	Mn_3O_4	0.5 wt% K/Mn_3O_4	0.5 wt% Ca/Mn_3O_4	0.5 wt% Mg/Mn_3O_4
Mn $2p_3$ (eV)	641.01	642.04	642.02	642.09
O 1s A (eV)	529.77	529.66	530.06	530.11
O 1s B (eV)	531.40	531.87	532.30	531.80
Area ratio of O 1s B/O 1s A	0.36	0.47	0.46	0.40

and Mg to Mn_3O_4 catalyst lead the BE to increase to 642.04, 642.02 and 642.09 eV, respectively. These BEs are the categories between the BE of Mn_2O_3 and Mn_3O_4. Accordingly, the increase in the BEs due to the additions of K, Ca and Mg seems to be strong evidence of the presence of a defect in manganese. As shown in Fig. 7, the oxygen O 1s spectra were fitted roughly with two peaks, O 1s A and O 1s B, representing two different kinds of surface species. O 1s A with BE from 529.7 to 530.1 eV is the characteristic of lattice oxide, while O 1s B with BE in the range of 531.4–532.3 eV belongs most likely to a defect-oxide or a hydroxyl-like group [30]. The 4th row of Table 1 lists the area ratios of O 1s B/O 1s A (the relative abundance of these two kinds of oxygen species). The area ratios of O 1s B/O 1s A of Mn_3O_4, and the promoted Mn_3O_4 catalysts with K, Ca and Mg are 0.36, 0.47, 0.46 and 0.40, respectively. Mn_3O_4 catalyst contained less O 1s B species than the promoted Mn_3O_4. In addition, as noticed in the catalytic activity, the promoted Mn_3O_4 catalyst has higher conversion than the Mn_3O_4 catalyst. Accordingly, an increase in the area ratio of O 1s B/O 1s A is well connected with an increase in toluene conversion. This strongly suggests that O 1s B species, which has higher mobility than lattice oxygen [31], can positively participate in the toluene oxidation and greatly contribute to the catalytic activity. This finding is in good accordance with the TPR data in Fig. 6. In other words, the increases in the area ratio of O 1s B/O 1s A are likely to correspond to the shoulder peaks in TPR profiles of the promoted Mn_3O_4 catalyst with K, Ca and Mg. This result indicates that K, Ca and Mg have an important role in the formation of O 1s B in Mn_3O_4 catalyst.

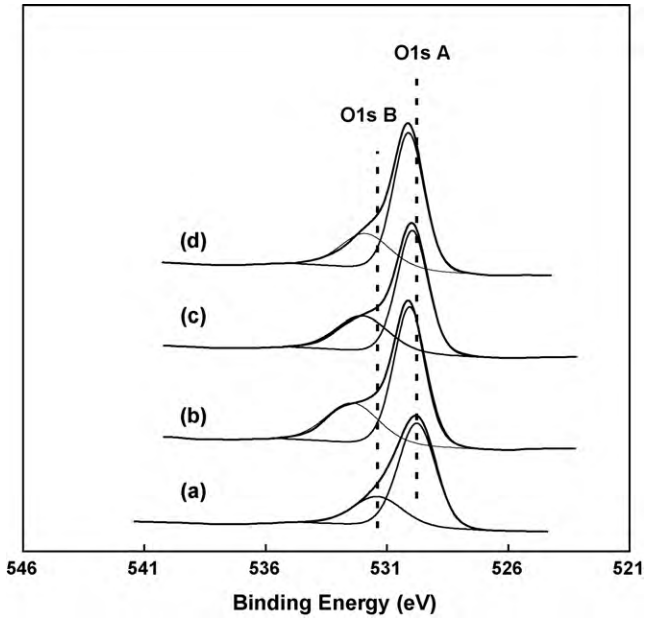

Fig. 8. XPS spectra of the O 1s region of samples. (a) Mn_3O_4, (b) 0.5 wt% K/Mn_3O_4, (c) 0.5 wt% Ca/Mn_3O_4, and (d) 0.5 wt% Mg/Mn_3O_4.

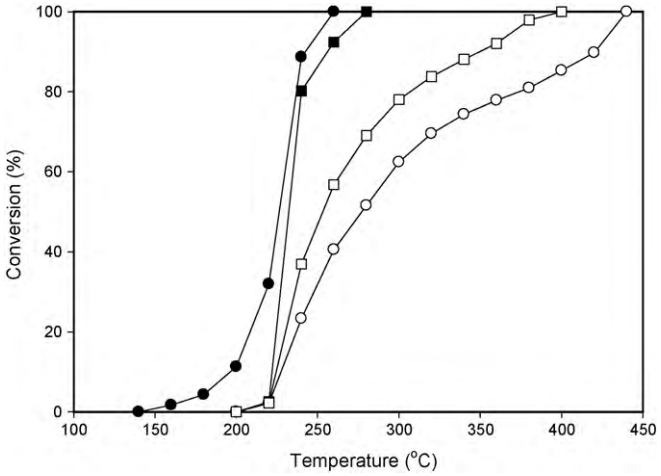

Fig. 9. Conversions of benzene, toluene or benzene and toluene in binary mixture over 0.5 wt% Ca/Mn_3O_4. *Reaction condition*: catalyst weight = 0.4 g; benzene or toluene concentration = 2000 ppm; the mixture concentration of benzene (1000 ppm) and toluene (1000 ppm) = 2000 ppm; total flow rate = 100 cm^3/min. (●) benzene; (■) toluene; (○) benzene in binary mixture; (□) toluene in binary mixture.

3.4. Oxidation of binary mixture

To evaluate the possible inhibitory effects in the oxidation reactions, we studied the single compound and binary mixture: benzene (2000 ppm), toluene (2000 ppm), benzene (1000 ppm) – toluene (1000 ppm). The conversion profiles for single compound (benzene, toluene) and binary mixture (benzene–toluene) over 0.5 wt% Ca/Mn_3O_4 catalyst are plotted in Fig. 9. The reaction temperatures for T_{50} (T_{90}) conversion of benzene and toluene for single compound are 225 (240) and 235 (260) °C, respectively, and those for T_{50} (T_{90}) conversion of benzene and toluene for binary mixture are 275 (420) and 250 (350) °C, respectively. As noticed in the catalytic activity test, mutual inhibitory effect between both compounds was observed in the mixture of benzene and toluene. Accordingly, there is probably a competitive reaction in the binary mixture. In other words, the reaction of the binary mixture (benzene and toluene) is a competitive one running on the same active sites. In addition, it should be noted that in the case of the single compound, benzene is more easily oxidized than toluene, and conversely, toluene is more easily oxidized than benzene in the binary mixture. Some researchers [32,33] have reported that the catalytic activity with respect to the VOC molecule was observed to follow the sequence of benzene > toluene, and the activity order followed the order of adsorption of each VOC, indicating that the oxidation rate is correlated with the surface VOC concentration. Accordingly, in the case of the single compound, benzene, not toluene, seems to easily adsorb on the catalyst: however, in the binary mixture, toluene appears to be more favorable to the active sites than benzene.

4. Conclusion

The catalytic combustion of VOCs (benzene and toluene) was carried out over manganese oxide catalysts (Mn_3O_4, Mn_2O_3 and MnO_2) and the promoted Mn_3O_4 catalysts with K, Ca and Mg. The catalytic activity according to each manganese oxide catalyst was in the order Mn_3O_4 > Mn_2O_3 > MnO_2. The TPR and the BET results

indicated that catalyst with high oxygen mobility and a high surface area exhibits high catalytic activity. The XPS and the TPR results also revealed that the addition of K, Ca and Mg causes a defect-oxide or a hydroxyl-like group, which may be responsible for enhancing the catalytic activity, to be formed on Mn_3O_4 catalyst, subsequently, leading to the enhancement of the catalytic activity of Mn_3O_4 catalyst. In the mixture of benzene and toluene, mutual inhibitory effect between both compounds was observed. Thus the reaction of benzene and toluene seemed to be a competitive one running on the same active sites. In addition, in the case of the single compound, benzene is more easily oxidized than toluene, and conversely, toluene is more easily oxidized than benzene in the binary mixture. Consequently, toluene appears to be more favorable to active sites than benzene in mixture.

Acknowledgement

This work was supported by the Korea Research Foundation Grant funded by the Korean Government (KRF-2008-313-D00537).

References

[1] J.A. Horsley, Catalytica Environmental Report No. E4, Catalytica Studies Division, Mountain View, CA, USA 1993.
[2] N. Li, F. Gaillard, Appl. Catal. B: Environ. 88 (2009) 152–159.
[3] F.N. Aguero, B.P. Barbero, L. Gambaro, L.E. Cadús, Appl. Catal. B: Environ. 91 (2009) 108–112.
[4] Y. Li, X. Zhang, H. He, Y. Yu, T. Yuan, Z. Tian, J. Wang, Y. Li, Appl. Catal. B: Environ. 89 (2009) 659–664.
[5] A.R. Gandhe, J.S. Rebello, J.L. Figueiredo, J.B. Fernandes, Appl. Catal. B: Environ. 72 (2007) 129–135.
[6] F. Diehl, J. Barbier Jr., D. Duprez, I. Guibard, G. Mabilon, Appl. Catal. B: Environ. 95 (2010) 217–227.
[7] K.J. Kim, H.G. Ahn, Appl. Catal. B: Environ. 91 (2009) 308–318.
[8] C. He, J. Li, P. Li, J. Cheng, Z. Hao, Z.P. Xu, Appl. Catal. B: Environ. 96 (2010) 466–475.
[9] W.G. Shim, J.W. Lee, S.C. Kim, Appl. Catal. B: Environ. 84 (2008) 133–141.
[10] J. Bedia, J.M. Rosas, J. Rodríguez-Mirasol, T. Cordero, Appl. Catal. B: Environ. 94 (2010) 8–18.
[11] S. Todorova, H. Kolev, J.P. Holgado, G. Kadinova, Ch. Bonev, R. Pereñíguez, A. Caballero, Appl. Catal. B: Environ. 94 (2010) 46–54.
[12] S.C. Kim, J. Hazard. Mater. B 91 (2002) 285–299.
[13] J.J. Spivey, J.B. Butt, Catal. Today 11 (1992) 465–590.
[14] V.H. Vu, J. Belkokuch, A. Ould-dris, B. Taouk, AIChE 54 (2008) 1585–1591.
[15] M. Baldi, E. Finocchio, G. Busca, Appl. Catal. B: Environ. 16 (1998) 43–51.
[16] M. Baldi, V.S. Escribano, J.M.G. Amores, F. Milella, G. Busca, Appl. Catal. B: Environ. 17 (1998) L175–L182.
[17] C. Lahousse, A. Bernier, P. Grange, B. Delmon, P. Papaefthimiou, T. Ioannides, X.V. Kios, J. Catal. 178 (1998) 214–225.
[18] K. Ramesh, L. Chen, F. Chen, Y. Liu, Z. Wang, Y.F. Han, Catal. Today 131 (2008) 477–482.
[19] V.P. Santos, M.F.R. Pereira, J.J.M. Órfão, J.L. Figueiredo, Top. Catal. 52 (2009) 470–481.
[20] R. Lin, W.P. Liu, Y.-J. Zhong, M.-F. Luo, Appl. Catal. A: Gen. 220 (2001) 165–171.
[21] A.H. Reidies, Ullmann's Encyclopedia of Industrial Chemistry, vol. A16, VCH, Weinheim, 1990, p. 123.
[22] T.K. Tseng, H. Chu, Sci. Total Environ. 275 (2001) 83–93.
[23] S.S.T. Bastos, J.J. Orfao, M.M.A. Freitas, M.F.R. Pereira, J.L. Figueiredo, Appl. Catal. B: Environ. 93 (2009) 30–37.
[24] K.M. Parida, A. Samal, Appl. Catal. A: Gen. 182 (1999) 249–256.
[25] Y. Yongnian, H. Ruili, C. Lin, Z. Jiayu, Appl. Catal. A: Gen. 101 (1993) 233–252.
[26] D. Jarosch, Miner. Petrol. 37 (1987) 15–23.
[27] L. Christel, A. Pierre, D.A.M.R. Abel, Thermochim. Acta 306 (1997) 51–59.
[28] S. Scirè, S. Minicò, C. Crisafulli, S. Galvagno, Catal. Commun. 2 (2001) 229–232.
[29] S.C. Kim, W.G. Shim, J. Hazard. Mater. 154 (2008) 310–316.
[30] B. Gillot, S. Buguet, E. Kester, C. Baubet, Ph. Tailhades, Thin Solid Films 357 (1999) 223–231.
[31] H. Chen, A. Sayari, A. Adnot, F. Larachi, Appl. Catal. B: Environ. 32 (2001) 195–204.
[32] J.C.S. Wu, Z.A. Lin, F.M. Tsai, J.W. Pan, Catal. Today 63 (2000) 419–426.
[33] W.G. Shim, S.C. Kim, Appl. Surf. Sci. 256 (2010) 5566–5571.